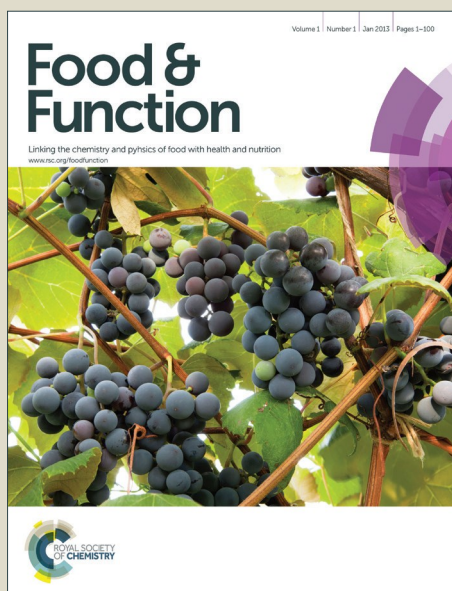


# Food & Function

Accepted Manuscript



This is an *Accepted Manuscript*, which has been through the Royal Society of Chemistry peer review process and has been accepted for publication.

*Accepted Manuscripts* are published online shortly after acceptance, before technical editing, formatting and proof reading. Using this free service, authors can make their results available to the community, in citable form, before we publish the edited article. We will replace this *Accepted Manuscript* with the edited and formatted *Advance Article* as soon as it is available.

You can find more information about *Accepted Manuscripts* in the [Information for Authors](#).

Please note that technical editing may introduce minor changes to the text and/or graphics, which may alter content. The journal's standard [Terms & Conditions](#) and the [Ethical guidelines](#) still apply. In no event shall the Royal Society of Chemistry be held responsible for any errors or omissions in this *Accepted Manuscript* or any consequences arising from the use of any information it contains.



29 **KEYWORDS:** Ginsenoside Re, Cardiac dysfunction, Endotoxin, Estrogen receptor.

30 **Abbreviations:**

31 Akt, Protein kinase B; AST, Aspartate transaminase; CK, Creatine kinase; EF, Ejection fraction;  
32 ERK1/2, Extracellular signal-regulated kinase 1 and 2; ER, Estrogenic hormone; FS, Fractional  
33 shortening; GS-Re, Ginsenoside Re; IFN- $\gamma$ , Interferon  $\gamma$ ; I-kB $\alpha$ , Inhibitory-kB $\alpha$ ; IL, Interleukin;  
34 iNOS, Inducible nitric oxide synthase; JNK, c-Jun N-terminal kinases; LDH, Lactate  
35 dehydrogenase; LPS, Lipopolysaccharide; LVIDs, Left ventricular internal diameter in systole;  
36 LVIDd, Left ventricular internal diameter in diastole; LVPWs, Left ventricular posterior wall  
37 thickness in systole; LVPWd, Left ventricular posterior wall thickness in diastole; LVVd, Left  
38 ventricular end-diastolic volume; LVVs, Left ventricular end-systolic volume; MAPK,  
39 Mitogen-activated protein kinase; MCP-1, membrane cofactor protein 1; NF-kB, Nuclear  
40 factor-kB; PI3K, Phosphatidylinositol 3-kinase; TLR, Toll-like receptor; TNF, Tumour necrosis  
41 factor.

42 **1. Introduction**

43 Severe sepsis and septic shock, also defined as a systemic inflammatory response to infection and  
44 progressive organ dysfunction, are among the most important causes of morbidity and mortality in  
45 hospitalized patients around the world [1]. Accumulating evidences suggest that the cardiovascular  
46 system is frequently affected by sepsis [2]. Cardiac dysfunction is a typical manifestation of  
47 sepsis/septic shock [3]. The prevention of cardiac dysfunction can significantly decrease the  
48 mortality of patients in sepsis/septic shock [1,2].

49 Ginseng (family Araliaceae) is a well-known medicinal plant that has been used in China for  
50 thousands of years to treat cancer, inflammation, stress, and diabetes [4]. Studies showed that the  
51 pharmacological and biological activities of ginseng are mainly attributed to ginsenosides, which  
52 are its most prominent and active components. As a major active ingredient, ginsenoside Re  
53 (GS-Re) possesses multifaceted pharmacological effects on the cardiovascular system [5]. GS-Re  
54 can alter cardiac electrophysiological properties, which may account for its antiarrhythmic effect  
55 [6]. Besides, GS-Re also exerts anti-ischemic effect and induces angiogenic regeneration [7].

56 Lipopolysaccharide (LPS) is a component of the outer membrane of mainly Gram-negative  
57 bacteria and the most important pathogen leading to sepsis development. Studies have  
58 demonstrated that LPS induced myocardial inflammation and dysfunction by interacting with its  
59 ligand TLR-4, thus triggering the activation of multiple signaling pathways, such as MAPKs  
60 family [8], NAD(P)H oxidase [9], and GSK3 $\beta$  [10]. Besides, LPS could induce an imbalance  
61 between eNOS and iNOS in the myocardium. This imbalance may be triggered by LPS challenge  
62 and/or proinflammatory cytokine overproduction [11]. LPS can also increase intracellular Ca<sup>2+</sup>  
63 concentrations [12]. All these signaling pathways can induce inflammatory response in  
64 cardiomyocyte [13]. LPS-induced inflammatory response serves an important function in the  
65 progression of cardiac dysfunction [2]. NF- $\kappa$ B is an important signal integrator that can be  
66 triggered by TLR-4 activation. NF- $\kappa$ B controls the production of many pro-inflammatory  
67 cytokines, such as tumor necrosis factor (TNF)- $\alpha$ , interleukin (IL)-1 $\beta$ , IL-6, monocyte chemotactic  
68 protein-1 (MCP-1), and the cytokine-inducible nitric oxide synthase (iNOS) [14,15]. NF- $\kappa$ B  
69 signaling pathway has an important function in myocardial dysfunction during sepsis. Inhibition of  
70 NF- $\kappa$ B can prevent LPS-induced cardiac dysfunction [16]. The activity of NF- $\kappa$ B can be regulated  
71 by phosphatidylinositide 3-kinase (PI3K)/protein kinase B (Akt) and mitogen-activated protein  
72 kinase (MAPK) [17,18].

73 Studies have shown that estrogen receptors (ERs) play an important role in endotoxin-induced  
74 cardiac dysfunction [19,20]. Clinical studies revealed that women have lower mortality rate and  
75 TNF- $\alpha$  level than men during sepsis [21]. ERs are important in limiting inflammatory response  
76 during sepsis/septic shock. GS-Re is a phytoestrogen and can exert pharmacological effects via  
77 regulating the activities of ERs [22]. GS-Re reportedly exhibits anti-inflammatory effects [23,24].  
78 Lee found that GS-Re could inhibit the binding of LPS to TLR4 on macrophages [25]. However,  
79 whether GS-Re protects the heart during sepsis/septic shock has not been investigated yet. The  
80 aim of the present study was to evaluate the effects of GS-Re on cardiac dysfunction during  
81 sepsis/septic shock in mice.

## 82 **2. Materials and methods**

### 83 **2.1. Chemicals and materials**

84 GS-Re with more than 98% purity was purchased from Shanghai Winherb Medical S & T  
85 Development Co., Ltd. (Shanghai, China). LPS (*Escherichia coli* O111:B4) was purchased from  
86 Sigma (St. Louis, MO, USA). The kit for determining lactate dehydrogenase (LDH), creatine  
87 kinase (CK), and aspartate aminotransferase (AST) were obtained from the Jiancheng  
88 Bioengineering Institute (Nanjing, China). Primary antibodies against TNF- $\alpha$ , IL-6, IL-1 $\beta$ , eNOS,  
89 iNOS, I- $\kappa$ B, p-p65, p-ERK, ERK, p-JNK, JNK, p-P38, P38, TLR4, p-AKT, AKT, ER $\alpha$ , ER $\beta$ ,  
90  $\beta$ -actin were from Santa Cruz Biotechnology (CA). Horseradish peroxidase (HRP)-conjugated  
91 secondary antibodies were from CWbiotech (Beijing, China). All other chemicals were purchased  
92 from Sigma (St. Louis, MO, USA). The purity of all chemical reagents was at least analytical  
93 grade, and all were commercially available.

## 94 **2.2 Experimental animals**

95 Male C57BL/6 mice (18 g to 20 g) were obtained from Beijing Vital River Laboratory Animal  
96 Technology Co., Ltd. (Beijing, China). The mice were acclimatized for 1 week before experiments.  
97 The environment was controlled at 24 °C to 25 °C room temperature, 55% humidity, and 12:12  
98 h light: dark cycle. This study was carried out in strict accordance with the recommendations in  
99 the Guide for the Care and Use of Laboratory Animals of the National Institutes of Health. The  
100 protocol was approved by the Committee on the Ethics of Animal Experiments of the Peking  
101 Union Medical College (Permit Number: #IMPLAD2012112207). All surgery was performed  
102 under sodium pentobarbital anesthesia, and all efforts were made to minimize suffering.

## 103 **2.3 Experimental design**

104 A total of 80 mice were randomly divided into four groups. Cont group: mice were dosed  
105 intragastrically with distilled water. Re group (distilled water dissolved): mice were dosed  
106 intragastrically with 15mg/kg GS-Re for 7 days. LPS group (normal saline dissolved): mice were  
107 treated with LPS intraperitoneal at a dose of 10 mg/kg. LPS + Re group: mice were treated with  
108 GS-Re for 7 days. At 1 h after the last administration, LPS were intraperitoneally injected. At 6 h  
109 after LPS administration, heart tissues were fixed in 4% buffered paraformaldehyde for histology  
110 and immunohistochemistry or were frozen at -80 °C for protein analyses. Another experiment was

111 conducted, and the survival rate of mice was monitored once every 2 h for up to 24 h. In a separate  
112 experiment, mice were pretreated with a non-selective ER antagonist, ICI 182780 (ICI; 2 mg/kg  
113 body weight) 1 h before LPS administration.

#### 114 **2.4 Echocardiographic measurements**

115 M-mode echocardiography was performed using Vevo 770™ High Resolution Imaging System  
116 (VisualSonics Inc., Canada). After treatment, the mice were anesthetized and their chests were  
117 shaved. The mice were then placed in recumbent position. Left ventricular (LV) internal diameter  
118 in systole (LVIDs) and diastole (LVIDd), and LV posterior wall thickness in systole (LVPWs) and  
119 diastole (LVPWd) were measured using M-mode echocardiography. LV end-diastolic volume  
120 (LVVd), LV end-systolic volume (LVVs), fractional shortening (FS), and ejection fraction (EF)  
121 were automatically calculated using an ultrasound machine.

#### 122 **2.5 Measurement the activity of LDH, CK and AST**

123 After the completion of the echocardiography, blood samples were obtained from the inner  
124 canthus using a capillary tube under chloral hydrate anesthesia. The samples were centrifuged at  
125 3000×g for 15 min within 1 h after collection. The activities of lactate dehydrogenase (LDH),  
126 creatine kinase (CK), and aspartate transaminase (AST) in the plasma were measured with the  
127 corresponding detection kit according to the manufacturers' instructions (Nanjing Jiancheng  
128 Bioengineering, China).

#### 129 **2.7 Histological and Immunohistochemical Analysis**

130 Heart tissues were fixed in 4% buffered paraformaldehyde, dehydrated in graded ethanol and then  
131 embedded in paraffin wax. The heart apex was sectioned, stained with hematoxylin and eosin  
132 (H&E), and then examined under a light microscope (CKX41, 170 Olympus, Tokyo, Japan).

133 For immunohistochemical analysis, slides were deparaffinized and hydrated. Endogenous  
134 peroxidases were blocked by hydrogen dioxide. Sections were incubated with goat anti-CD 68  
135 monoclonal antibody and then stained using 3, 3'-diaminobenzidine kit. Finally, slides were

136 re-stained with hematoxylin and observed by light microscopy.

### 137 **2.8 Measurement the activity of TNF- $\alpha$ , IL-1 $\beta$ , IL-6, IFN- $\gamma$ , MCP-1, and IL-10**

138 Heart tissues were mixed with saline at a ratio of 1:9 (mg/ $\mu$ L) to form a homogenate. After  
139 centrifugation at 7000 rpm for 5 min, the supernatant was used to measure the levels of TNF- $\alpha$ ,  
140 IL-1 $\beta$ , IL-6, IFN- $\gamma$ , MCP-1, and IL-10 by ELISA according to the manufacturer's instructions  
141 (R&D Systems, Wiesbaden, Germany).

### 142 **2.9 Western Blot Analysis**

143 Heart tissues were mixed with saline at a ratio of 1:9 (mg/ $\mu$ L) to form a homogenate. After  
144 centrifugation at 7000 rpm for 5 min, the precipitate was lysed on ice with tissue-protein  
145 extraction reagent containing 0.1 mM dithiothreitol and proteinase inhibitor cocktail. Protein  
146 concentration was determined using a BCA kit (Pierce Corporation, Rockford, USA). An  
147 equivalent amount of protein was added, and the mixture was loaded onto 12%  
148 SDS-polyacrylamide gels (Mini-PROTEAN II, Bio-Rad), separated, and transferred to  
149 nitrocellulose membranes. The membranes were blocked with 5% (w/v) non-fat milk powder in  
150 tris-buffer containing 0.05% (v/v) Tween-20 (TBST) for 2 h at room temperature. After overnight  
151 incubation with the appropriate primary antibodies at 4 °C, the membranes were washed thrice  
152 with TBST and incubated with secondary antibodies for 2 h at room temperature before  
153 re-washing thrice with TBST. The protein blots were developed using an enhanced  
154 chemiluminescence solution. Protein expression levels were visualized with Image Lab Software  
155 (Bio-Rad, USA).

### 156 **2.10 Statistical Analysis**

157 Results from at least three independent experiments were expressed as mean  $\pm$  SE. Statistical  
158 comparisons between different groups were measured with Student's t-test or ANOVA using Prism  
159 5.00 software. Statistical significance was considered at  $p < 0.05$ .

## 160 **3. Results**

---

### 161 **3.1 Effects of GS-Re on survival rate of LPS-treated mice**

162 We first evaluated the effects of GS-Re on sepsis-induced mortality. After LPS treatment, animal  
163 survival was monitored for up to 24 h. As shown in Figure 1B, mice began to die at 8 h after the  
164 LPS-treatment. However, mice in LPS+Re group exhibited significantly longer survival compared  
165 with the mice in LPS group. No mouse died within 6 h. Therefore, the mice treated with LPS for 6  
166 h were used in the subsequent experiments.

### 167 **3.2 Effects of GS-Re on heart function of LPS-treated mice**

168 To investigate the effect of GS-Re on cardiac function of LPS-treated mice, M-mode  
169 echocardiography was used to measure cardiac parameters. Compared with control group, LPS  
170 administration significantly decreased ejection fraction (EF), fractional shortening (FS), left  
171 ventricular internal diameter at diastolic phase (LVDd), and left ventricular internal diameter at  
172 systolic phase (LVDs). GS-Re pretreatment attenuated LPS-induced cardiac dysfunction in mice  
173 (Figures 2A and 2B).

174 LDH, CK, and AST are three important indicators of cardiac injury. As shown in Figure 2C, LPS  
175 significantly increased the serum levels of LDH, CK, and AST, which was suppressed by  
176 pretreatment with GS-Re.

### 177 **3.4 Effects of GS-Re on LPS-induced heart damage**

178 H&E staining indicated that LPS administration significantly increased erythrocyte leakage and  
179 leukocyte infiltration into the cardiac interstitium (Figure 3A). Moreover, the number of CD  
180 68-positive cells, representing monocyte/macrophage in an activated state, increased in the heart  
181 tissues after the LPS challenge (Figure 3B). GS-Re pretreatment obviously attenuated  
182 LPS-induced neutrophil/leukocyte infiltration.

### 183 **3.5 Effects of GS-Re on inflammatory cytokine production in LPS-treated mice**

184 The protein levels of TNF- $\alpha$ , IL-1 $\beta$  and IL-6 in cardiac tissues of mice significantly increased in  
185 the LPS group compared with the control group. This increase was significantly attenuated by

186 GS-Re pretreatment. No significant difference was found between saline- and GS-Re-treated mice  
187 (Figures 4A and 4B). ELISA was used to determine the levels of inflammatory cytokine in  
188 response to LPS stimulation. The levels of TNF- $\alpha$ , IL-1 $\beta$ , IL-6, INF- $\gamma$ , MCP-1, and IL-10 in  
189 cardiac tissues of LPS-treated mice increased significantly compared with those in the  
190 saline-treated controls. In contrast, GS-Re pretreatment significantly attenuated the increase of  
191 TNF- $\alpha$ , IL-1 $\beta$ , IL-6, INF- $\gamma$ , and MCP-1 levels induced by LPS. However, the level of IL-10  
192 increased further after GS-Re pretreatment (Figure 4C).

### 193 **3.6 Effects of GS-Re on LPS-induced imbalance between eNOS and iNOS in mice**

194 An imbalance between iNOS and eNOS serves an important function in myocardial dysfunction  
195 during sepsis. LPS administration significantly decreased the level of eNOS and increased the  
196 level of iNOS compared with the control group, which was significantly attenuated by GS-Re  
197 pretreatment (Figure 5A). No significant difference was found between the control group and the  
198 Re group.

### 199 **3.7 Effects of GS-Re on NF- $\kappa$ B signaling pathway**

200 NF- $\kappa$ B signaling pathway in myocardial tissue is activated after cardiac dysfunction during  
201 sepsis/septic shock. In our study, LPS administration significant increased I $\kappa$ B- $\alpha$  degradation and  
202 NF- $\kappa$ B p65 phosphorylation. By contrast, GS-Re pretreatment significantly attenuated I $\kappa$ B- $\alpha$   
203 degradation and p65 phosphorylation as opposed to the LPS group (Figure 5B). No significant  
204 difference was found between the control group and Re group.

### 205 **3.8 Effects of GS-Re on MAPK signaling pathway**

206 MAPK signaling pathway has an important function in modulating the NF- $\kappa$ B signaling pathway.  
207 As shown in Figure 8, LPS stimulation significantly increased phosphorylation of JNK, ERK, and  
208 p38 MAPK in comparison to the control group. GS-Re pretreatment dramatically inhibited the  
209 phosphorylation of JNK, ERK, and p38 MAPK (Figure 6). These results demonstrated that GS-Re  
210 inhibited the activity of MAPK pathways in LPS-induced endotoxemia.

---

### 211 3.9 Effects of GS-Re on TLR4, ERs, and phospho-Akt

212 As shown in Figure 7, GS-Re significantly increased ER $\alpha$  and ER $\beta$  expression in the LPS+Re and  
213 the Re groups. The PI3K/AKT is a downstream signaling pathway of ERs that plays a key role in  
214 cardiac dysfunction during sepsis/septic shock. As shown in Figure 7, LPS administration  
215 significantly reduced the level of phospho-Akt compared with control group, which was preserved  
216 by GS-Re pretreatment. These results suggested that GS-Re may attenuate LPS-induced NF- $\kappa$ B  
217 activation and inflammation response partially through ERs and PI3K signaling. However, GS-Re  
218 had no obvious effect on the LPS-induced up-regulation of TLR-4 (Figure 7).

### 219 3.10 ERs inhibition abolished the protective effect of GS-Re on LPS-induced cardiac 220 dysfunction

221 To assess further whether ERs were associated with the cardioprotective properties of GS-Re, we  
222 evaluated cardiac function in mice by echocardiography upon stimulation with LPS, GS-Re, or  
223 pharmacological inhibitor. Figures 8A show that non-selective (ICI 182780) ERs antagonist  
224 decreased EF, FS, LVDd, and LVDs in GS-Re and LPS co-treated mice. Importantly, this  
225 pharmacological inhibitor abolished the suppression of GS-Re on the production of  
226 proinflammatory cytokines in LPS-induced sepsis (Figures 8B).

### 227 4. Discussion

228 In the present study, GS-Re was proved for the first time to reduce LPS-induced cardiac  
229 dysfunction in mouse. We observed that GS-Re significantly decreased the serum levels of CK,  
230 LDH, and AST in LPS-treated mice and inhibited LPS-induced neutrophil/leukocyte infiltration  
231 into the myocardium. GS-Re ameliorated the imbalance between iNOS and eNOS, prevented  
232 NF- $\kappa$ B activation and the subsequent myocardial inflammatory. The mechanism underlying the  
233 cardioprotective effect of GS-Re may have depended on the inhibition of MAPK signaling  
234 pathway and activation of ERs and PI3K/Akt.

235 Cardiac dysfunction during sepsis/septic shock is always accompanied by neutrophil/leukocyte  
236 infiltration [1]. Our study showed that LPS administration significantly increased

237 neutrophil/leukocyte infiltration in the myocardium. By contrast, this pathological change was  
238 significantly inhibited by GS-Re pretreatment. In LPS-treated mice, we can see an elevation of  
239 pro-inflammatory cytokines, such as TNF- $\alpha$ , IL-1 $\beta$ , IL-6, IFN- $\gamma$ , and MCP-1 and  
240 anti-inflammatory cytokine IL-10. Pre-treatment with GS-Re decreased the level of TNF- $\alpha$ , IL-1 $\beta$ ,  
241 IL-6, IFN- $\gamma$ , and MCP-1, surprisingly, increased the level of IL-10. These pro-inflammatory  
242 cytokines are major triggers of cardiac dysfunction in endotoxin [1]. As a potent  
243 anti-inflammatory cytokine, IL-10 controls the degree and duration of the inflammatory response.  
244 An enhancement of IL-10 production is effective for the treatment of septic shock [26].

245 In our study, LPS significantly increased iNOS expression and reduced eNOS expression. Studies  
246 indicated that constitutively expressed eNOS has beneficial effects on myocardial function during  
247 sepsis. However, iNOS may induce deterioration of cardiac cells [27]. Interestingly, GS-Re  
248 pretreatment significantly inhibited the induction of iNOS and maintained normal eNOS levels  
249 following the LPS challenge. Our data suggested that a balance between eNOS and iNOS was  
250 important in the cardioprotective effect of GS-Re during endotoxemia.

251 NF- $\kappa$ B prominently regulates most inflammatory genes and controls the production of many  
252 pro-inflammatory cytokines [15]. Under normal conditions, NF- $\kappa$ B is sequestered in the cytoplasm  
253 by I $\kappa$ B- $\alpha$ . Following phosphorylation by I $\kappa$ B kinases, I- $\kappa$ B $\alpha$  was subsequently ubiquitinated and  
254 degraded. The degradation of I- $\kappa$ B $\alpha$  releases the NF- $\kappa$ B from I $\kappa$ B- $\alpha$ . NF- $\kappa$ B enters nuclear and  
255 binds to NF- $\kappa$ B promoter elements, thereby resulting in the activation of target genes expression  
256 [28]. Substantial evidence indicates that LPS induced myocardial inflammation and dysfunction  
257 by interacting with its ligand TLR4 on cardiomyocytes, thereby activating NF- $\kappa$ B signaling  
258 pathway [15]. LPS induced a significant degradation of I- $\kappa$ B $\alpha$  and activation of NF- $\kappa$ B in the heart,  
259 which was blocked by pretreatment with GS-Re. However, GS-Re pretreatment could not  
260 attenuate the protein level of TLR-4 after the LPS challenge. Hence, GS-Re-induced NF- $\kappa$ B  
261 inactivation and less inflammatory cytokine release may not be directly mediated by TLR-4.

262 MAPK family serves an important function in LPS-induced inflammatory response, thereby  
263 contributing to the development of septic cardiac dysfunction [29]. MAPK family can modulate  
264 the activity of NF- $\kappa$ B and the production of inflammatory factor. A previous study suggested that

265 the activation of ERK1/2, JNK, and p38 is required for LPS-induced TNF $\alpha$  expression [18].  
266 Therefore, GS-Re may have inhibited inflammatory mediators by inactivating the MAPK pathway.  
267 Here, we demonstrated that GS-Re indeed decreased the levels of p-ERK1/2, p-JNK, and p-p38 in  
268 LPS-treated mice.

269 ERs are implicated in many pathophysiological processes and serve an important function in  
270 cellular survival by regulating the PI3K/Akt pathway [30]. The nuclear localization and activity of  
271 phospho-Akt in the myocardium is higher in females than in age-matched men [31]. ER $\alpha$  can  
272 inhibit cardiomyocyte apoptosis through the activation of Akt [32]. GS-Re could increase the  
273 expression of ER $\alpha$  and ER $\beta$  and the level of phospho-Akt in the myocardium, which may have  
274 negatively regulated the LPS-induced, NF- $\kappa$ B-dependent inflammatory responses. Importantly,  
275 these findings were supported by the pharmacologic inhibition of ERs (by ICI) resulting in the  
276 abolished protection of GS-Re against LPS-induced cardiac dysfunction as well as abrogated  
277 GS-Re-inhibited the level of proinflammatory cytokines following LPS challenge. The data  
278 suggests that GS-Re, as a novel phytoestrogen, promotes ERs expression via an unknown  
279 mechanism. MAPK signaling pathway can also be regulated by ER activation. 17 $\beta$ -Estradiol  
280 prevents smooth muscle cell proliferation and migration by inhibiting p38 MAPK activation,  
281 whereas it promotes these events in endothelial cells [33]. However, the specific contributions of  
282 ER $\alpha$  and ER $\beta$  on these events remain require further study.

283 Although GS-Re pretreatment significantly inhibited the LPS-induced cardiac dysfunction and  
284 inflammatory reactions in mice, the results cannot be translated to a septic patient admitted to a  
285 hospital primarily because the current study is that of prevention. In addition, the duration of the  
286 experiment was only 6 h, and GS-Re did not completely prevent the adverse events associated  
287 with endotoxemia. Thus, the therapeutic functions of GS-Re on sepsis-related mortality have yet  
288 to be determined in future studies. Besides, six metabolites of GS-Re are detected in rat feces after  
289 oral administration by HPLC-ESI-MS/MS analysis. Their structures are identified as  
290 20(S)-ginsenoside Rg2, 20(S)-ginsenoside Rh1, 20(R)-ginsenoside Rh1, ginsenoside F1,  
291 3-oxo-ginsenoside Rh1 and protopanaxatriol [34]. So, it is interesting to study the  
292 pharmacological action of metabolites of GS-Re.

---

**293 Conclusion**

294 In summary, pretreatment with GS-Re attenuated LPS-induced myocardial inflammatory  
295 cytokines production, the imbalance between iNOS and eNOS, and NFκB activation, as well as  
296 improved myocardial dysfunction and reduced myocardial injury during endotoxemia. The  
297 mechanisms by which GS-Re attenuated cardiac dysfunction involve the inhibition of MAPK and  
298 preserved activation of ERs and the PI3K/Akt signaling pathway. However, more advanced  
299 research is necessary to further explore the mechanisms underlying GS-Re's protective effects  
300 against LPS-induced myocardial dysfunction.

**301 Acknowledgement**

302 This study was supported by the National Natural Science Foundation of China (Grant  
303 no.81173589), the Major Scientific and Technological Special Project for Significant New Drugs  
304 Formulation (Grant nos. 2010ZX09401-305-47, 2010ZX09401-305-21, and  
305 2012ZX09501001-004), and the Key Scientific and Technological Project of Jilin Province (Grant  
306 no. 11ZDGG008)

307 **Conflict of interest:** The authors declare no conflict of interest.

**308 Reference**

- 309 1. Zanotti-Cavazzoni SL, Hollenberg SM (2009) Cardiac dysfunction in severe sepsis and septic shock.  
310 *Curr Opin Crit Care* 15: 392-397.
- 311 2. Merx MW, Weber C (2007) Sepsis and the heart. *Circulation* 116: 793-802.
- 312 3. Jiang S, Zhu W, Li C, Zhang X, Lu T, et al. (2013) alpha-Lipoic acid attenuates LPS-induced cardiac  
313 dysfunction through a PI3K/Akt-dependent mechanism. *Int Immunopharmacol* 16: 100-107.
- 314 4. Jang H-J, Han I-H, Kim Y-J, Yamabe N, Lee D, et al. (2014) Anticarcinogenic Effects of Products of  
315 Heat-Processed Ginsenoside Re, a Major Constituent of Ginseng Berry, on Human Gastric  
316 Cancer Cells. *Journal of Agricultural and Food Chemistry* 62: 2830-2836.
- 317 5. Peng L, Sun S, Xie LH, Wicks SM, Xie JT (2012) Ginsenoside Re: pharmacological effects on  
318 cardiovascular system. *Cardiovasc Ther* 30: e183-188.
- 319 6. Wang YG, Zima AV, Ji X, Pabbidi R, Blatter LA, et al. (2008) Ginsenoside Re suppresses  
320 electromechanical alternans in cat and human cardiomyocytes. *Am J Physiol Heart Circ*  
321 *Physiol* 295: H851-859.
- 322 7. Lim KH, Lim DJ, Kim JH (2013) Ginsenoside-Re ameliorates ischemia and reperfusion injury in the  
323 heart: a hemodynamics approach. *J Ginseng Res* 37: 283-292.
- 324 8. He X, Wei Z, Zhou E, Chen L, Kou J, et al. (2015) Baicalein attenuates inflammatory responses by

- 325 suppressing TLR4 mediated NF- $\kappa$ B and MAPK signaling pathways in LPS-induced mastitis in  
326 mice. *International Immunopharmacology* 28: 470-476.
- 327 9. Kim J-S, Yeo S, Shin D-G, Bae Y-S, Lee J-J, et al. (2010) Glycogen synthase kinase 3 $\beta$  and  
328  $\beta$ -catenin pathway is involved in toll-like receptor 4-mediated NADPH oxidase 1  
329 expression in macrophages. *FEBS Journal* 277: 2830-2837.
- 330 10. Coant N, Simon-Rudler M, Gustot T, Fasseu M, Gandoura S, et al. (2011) Glycogen synthase  
331 kinase 3 involvement in the excessive proinflammatory response to LPS in patients with  
332 decompensated cirrhosis. *J Hepatol* 55: 784-793.
- 333 11. Tatsumi T, Akashi K, Keira N, Matoba S, Mano A, et al. (2004) Cytokine-induced nitric oxide  
334 inhibits mitochondrial energy production and induces myocardial dysfunction in  
335 endotoxin-treated rat hearts. *J Mol Cell Cardiol* 37: 775-784.
- 336 12. Wheeler M, Stachlewitz RF, Yamashina S, Ikejima K, Morrow AL, et al. (2000) Glycine-gated  
337 chloride channels in neutrophils attenuate calcium influx and superoxide production. *FASEB J*  
338 14: 476-484.
- 339 13. Zhang T, Feng Q (2010) Nitric oxide and calcium signaling regulate myocardial tumor necrosis  
340 factor-alpha expression and cardiac function in sepsis. *Can J Physiol Pharmacol* 88: 92-104.
- 341 14. Guolong Z, Ghosh S (2000) Molecular mechanisms of NF- $\kappa$ B activation induced by bacterial  
342 lipopolysaccharide through Toll-like receptors. *Journal of Endotoxin Research* 6: 453-457.
- 343 15. Kawai T, Akira S (2007) Signaling to NF- $\kappa$ B by Toll-like receptors. *Trends in Molecular Medicine*  
344 13: 460-469.
- 345 16. Haudek SB, Spencer E, Bryant DD, White DJ MD, JW. H (2001) Overexpression of cardiac  
346 I-kappaB $\alpha$  prevents endotoxin-induced myocardial dysfunction. *Am J Physiol Heart Circ*  
347 *Physiol* 280: H962-968.
- 348 17. Huang GJ, Deng JS, Chen CC, Huang CJ, Sung PJ, et al. (2014) Methanol extract of *Antrodia*  
349 *camphorata* protects against lipopolysaccharide-induced acute lung injury by suppressing  
350 NF-kappaB and MAPK pathways in mice. *J Agric Food Chem* 62: 5321-5329.
- 351 18. Frazier WJ, Xue J, Luce WA, Liu Y (2012) MAPK signaling drives inflammation in  
352 LPS-stimulated cardiomyocytes: the route of crosstalk to G-protein-coupled receptors. *PLoS*  
353 *One* 7: e50071.
- 354 19. Mahmoodzadeh S, Leber J, Zhang X, Jaisser F, Messaoudi S, et al. (2014) Cardiomyocyte-specific  
355 Estrogen Receptor Alpha Increases Angiogenesis, Lymphangiogenesis and Reduces Fibrosis  
356 in the Female Mouse Heart Post-Myocardial Infarction. *J Cell Sci Ther* 5: 153.
- 357 20. Arnal JF, Valera MC, Payrastra B, Lenfant F, Gourdy P (2012) Structure-function relationship of  
358 estrogen receptors in cardiovascular pathophysiological models. *Thromb Res* 130 Suppl 1:  
359 S7-11.
- 360 21. Schroder J, Kahlke V, Staubach K, Zabel P, Stuber F (1998) Gender differences in human sepsis.  
361 *Arch Surg* 133: 1200-1205.
- 362 22. Nakaya Y, Mawatari K, Takahashi A, Harada N, Hata A, et al. (2007) The phytoestrogen  
363 ginsenoside Re activates potassium channels of vascular smooth muscle cells through  
364 PI3K\_Akt and nitric oxide pathways. *J Med Invest* 54: 381-384.
- 365 23. Kang-Woo L, So Young J, Sun-Mi C, Eun Jin Y (2012) Effects of ginsenoside Re on LPS-induced  
366 inflammatory mediators in BV2 microglial cells. *BMC Complementary and Alternative*  
367 *Medicine* 12: 196.
- 368 24. Paul S, Shin HS, Kang SC (2012) Inhibition of inflammations and macrophage activation by

- 369 ginsenoside-Re isolated from Korean ginseng (*Panax ginseng* C.A. Meyer). *Food Chem*  
370 *Toxicol* 50: 1354-1361.
- 371 25. Lee IA, Hyam SR, Jang SE, Han MJ, Kim DH (2012) Ginsenoside Re ameliorates inflammation by  
372 inhibiting the binding of lipopolysaccharide to TLR4 on macrophages. *J Agric Food Chem* 60:  
373 9595-9602.
- 374 26. Saraiva M, O'Garra A (2010) The regulation of IL-10 production by immune cells. *Nat Rev*  
375 *Immunol* 10: 170-181.
- 376 27. Eddy FB (2005) Role of nitric oxide in larval and juvenile fish. *Comp Biochem Physiol A Mol*  
377 *Integr Physiol* 142: 221-230.
- 378 28. Frantz S, Hu K, Bayer B, Gerondakis S, Strotmann J, et al. (2006) Absence of NF-kappaB subunit  
379 p50 improves heart failure after myocardial infarction. *FASEB J* 20: 1918-1920.
- 380 29. Yang P, Han Y, Gui L, Sun J, Chen YL, et al. (2013) Gastrodin attenuation of the inflammatory  
381 response in H9c2 cardiomyocytes involves inhibition of NF-kappaB and MAPKs activation  
382 via the phosphatidylinositol 3-kinase signaling. *Biochem Pharmacol* 85: 1124-1133.
- 383 30. Sun B, Xiao J, Sun XB, Wu Y (2013) Notoginsenoside R1 attenuates cardiac dysfunction in  
384 endotoxemic mice: an insight into oestrogen receptor activation and PI3K/Akt signalling. *Br J*  
385 *Pharmacol* 168: 1758-1770.
- 386 31. Camper-Kirby D, Welch S, Walker A, Shiraishi I, Setchell K, et al. (2001) Myocardial Akt  
387 activation and gender: increased nuclear activity in females versus males. *Circ Res* 88:  
388 1020-1027.
- 389 32. Liu CJ, Lo JF, Kuo CH, Chu CH, Chen LM, et al. (2009) Akt mediates 17beta-estradiol and/or  
390 estrogen receptor-alpha inhibition of LPS-induced tumor necrosis factor-alpha expression and  
391 myocardial cell apoptosis by suppressing the JNK1/2-NFkappaB pathway. *J Cell Mol Med* 13:  
392 3655-3667.
- 393 33. Geraldes P (2002) Estrogen Regulation of Endothelial and Smooth Muscle Cell Migration and  
394 Proliferation: Role of p38 and p42/44 Mitogen-Activated Protein Kinase. *Arteriosclerosis,*  
395 *Thrombosis, and Vascular Biology* 22: 1585-1590.
- 396 34. G. Chen, M. Yang, Guo. D (2009) Metabolic study of ginsenoside Re in rats. *China J Chin Materia*  
397 *Med* 34: 1540-1543.
- 398

### 399 **Figure legends**

400 **Figure 1** (A) Molecular structure of GS-Re. (B) Effects of GS-Re on mice survival rate.

401 **Figure 2** Effects of GS-Re on left ventricular functions in mice. (A) Representative images of M-mode  
402 echocardiogram. (B) Echocardiography values are expressed as mean  $\pm$  SD. EF, ejection fraction; FS, fractional  
403 shortening; LVVd, left ventricular end-diastolic volume; LVVs, left ventricular end-systolic volume. (C) Effects of  
404 GS-Re on myocardial enzyme activities in LPS-treated mice. The results were expressed as the mean  $\pm$  SD of three  
405 independent experiments. \* indicates significant differences from the control ( $P < 0.05$ ). # indicates significant  
406 differences from treatment with LPS alone ( $P < 0.05$ ).

407 **Figure 3** Effects of GS-Re on neutrophil/leukocyte infiltration. After LPS treatment, hearts were harvested and  
408 sectioned for HE counterstaining (A) or immunohistochemistry (B). Infiltrated leukocytes or CD68-positive cells  
409 were examined under a microscope. The results were expressed as the mean  $\pm$  SD of three independent  
410 experiments. \* indicates significant differences from the control ( $P < 0.05$ ). # indicates significant differences from  
411 treatment with LPS alone ( $P < 0.05$ ).

412 **Figure 4** Effects of GS-Re on the levels of inflammatory cytokines in LPS-treated mice. (A) Myocardial TNF $\alpha$ ,  
413 IL-1 $\beta$ , and IL-6 expressions were assayed by Western blot analysis. (B) Quantification of protein expression. (C)  
414 The levels of TNF- $\alpha$ , IL-1 $\beta$ , IL-6, MCP-1, IFN- $\gamma$ , and IL-10 in heart tissues of mice were measured by ELISA. The  
415 results were expressed as the mean  $\pm$  SD of three independent experiments. \* indicates significant differences from  
416 the control ( $P < 0.05$ ). # indicates significant differences from treatment with LPS alone ( $P < 0.05$ ).

417 **Figure 5** Effects of GS-Re on the levels of eNOS, iNOS and NF- $\kappa$ B activation. (A) Protein levels of eNOS and  
418 iNOS in the myocardium, as examined by Western blot analysis (B) Protein levels of I $\kappa$ B and p-P65 in the  
419 myocardium, as examined by Western blot analysis. The results were expressed as the mean  $\pm$  SD of three  
420 independent experiments. \* indicates significant differences from the control ( $P < 0.05$ ). # indicates significant  
421 differences from treatment with LPS alone ( $P < 0.05$ ).

422 **Figure 6** Effects of GS-Re on the expression of phosphorylation of ERK1/2, JNK, and P38. The Protein levels of  
423 phospho-ERK, phospho-JNK, and phospho-P38 in the myocardium were examined by Western blot analysis. The  
424 results were expressed as the mean  $\pm$  SD of three independent experiments. \* indicates significant differences from  
425 the control ( $P < 0.05$ ). # indicates significant differences from treatment with LPS alone ( $P < 0.05$ ).

426 **Figure 7** Effects of GS-Re on the expression of TLR-4, ER $\alpha$ , ER $\beta$  and phosphorylation of AKT. The protein levels  
427 of TLR-4, ER $\alpha$ , ER $\beta$ , and the phosphorylation of AKT in the myocardium were examined by Western blot analysis.  
428 The results were expressed as the mean  $\pm$  SD of three independent experiments. \* indicates significant differences  
429 from the control ( $P < 0.05$ ). # indicates significant differences from treatment with LPS alone ( $P < 0.05$ ).

430 **Figure 8** Effect of ERs inhibition on the protective effects of GS-Re against LPS-induced cardiac dysfunction. (A)  
431 EF, ejection fraction; FS, fractional shortening; LVVd, left ventricular end-diastolic volume; LVVs, left ventricular  
432 end-systolic volume were automatically calculated by the ultrasound machine. (B) The levels of TNF- $\alpha$ , IL-1 $\beta$ ,  
433 IL-6, MCP-1, IFN- $\gamma$ , and IL-10 in heart tissues of mice were measured by ELISA. The results were expressed as

434 the mean  $\pm$  SD of three independent experiments. \* indicates significant differences from the control ( $P < 0.05$ ). #  
435 indicates significant differences from treatment with LPS alone ( $P < 0.05$ ). <sup>S</sup> indicates significant differences from  
436 GS-Re and LPS co-treatment ( $P < 0.05$ ).

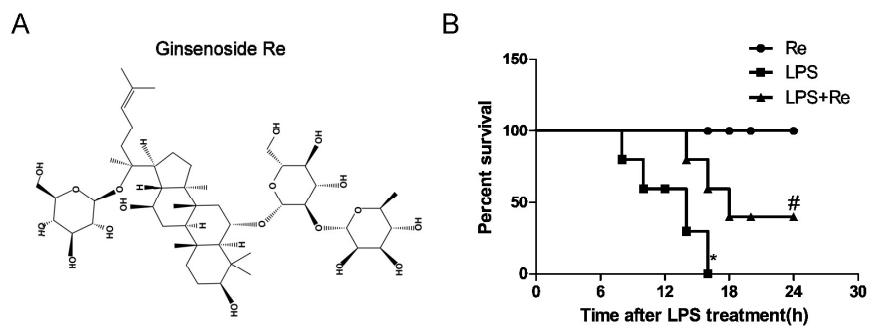
437

438

439

440

441

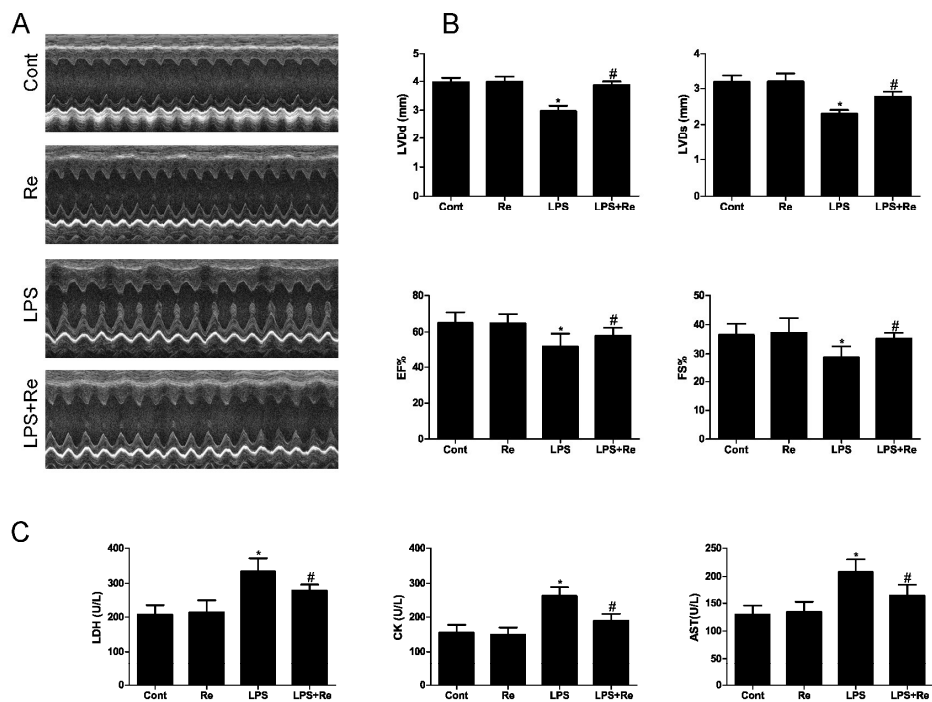
442 **Figure 1**

443

444

445

446 **Figure 2**



447

448

449

450

451

452

453

454

455

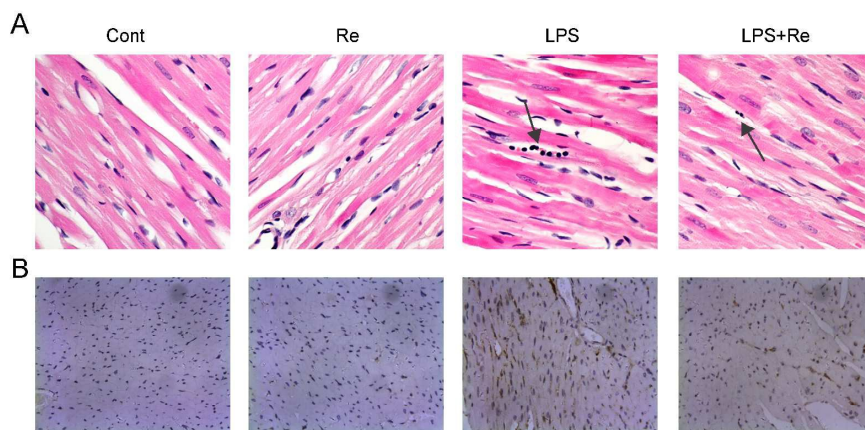
456

457

458

459

Figure 3



460

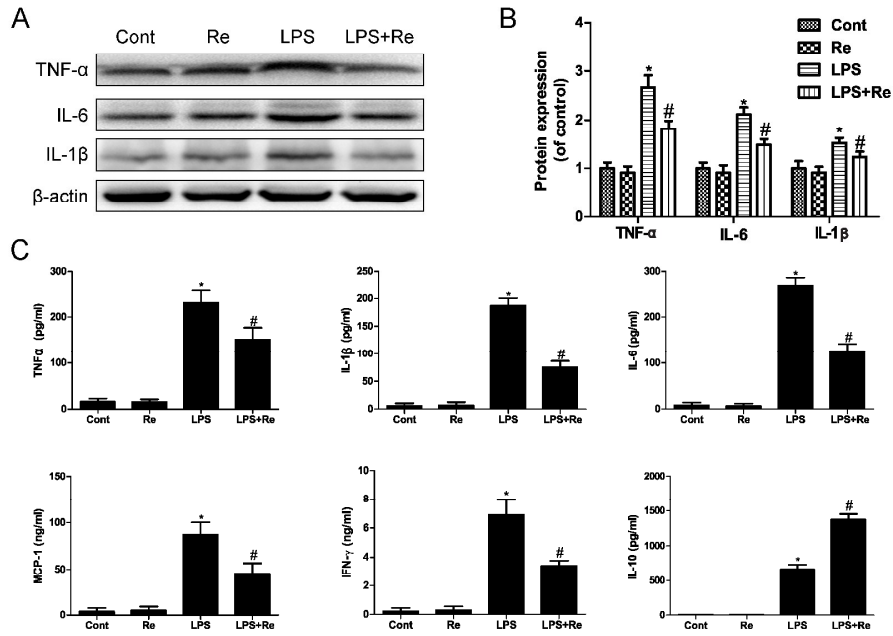
461

462

463

464

**Figure 4**



465

466

467

468

469

470

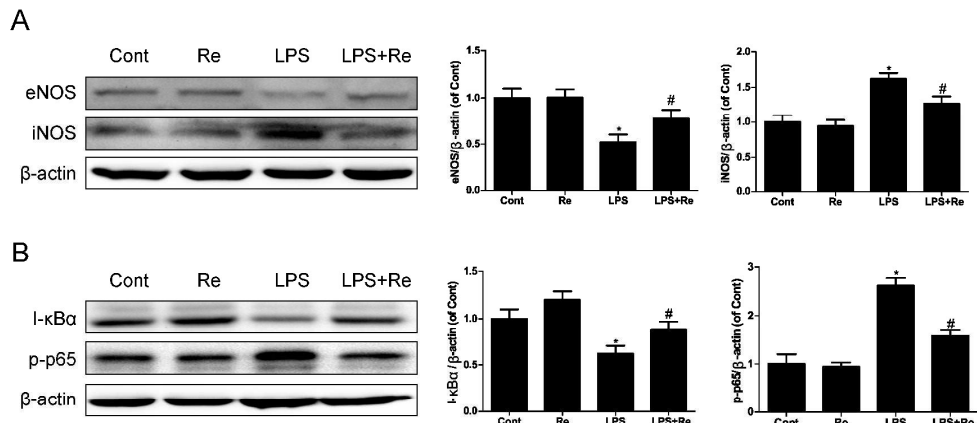
471

472

473

474

**Figure 5**



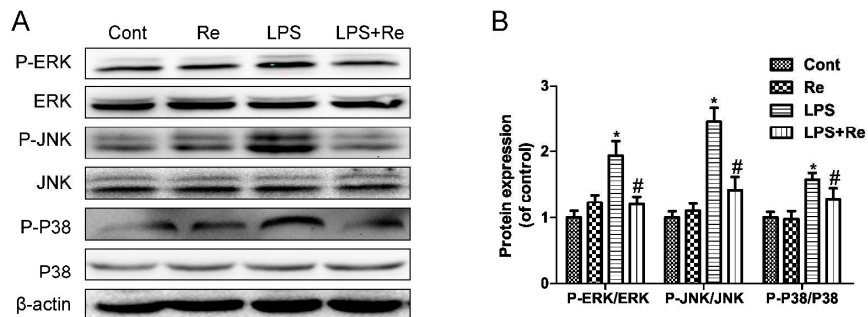
475

476

477

478

479

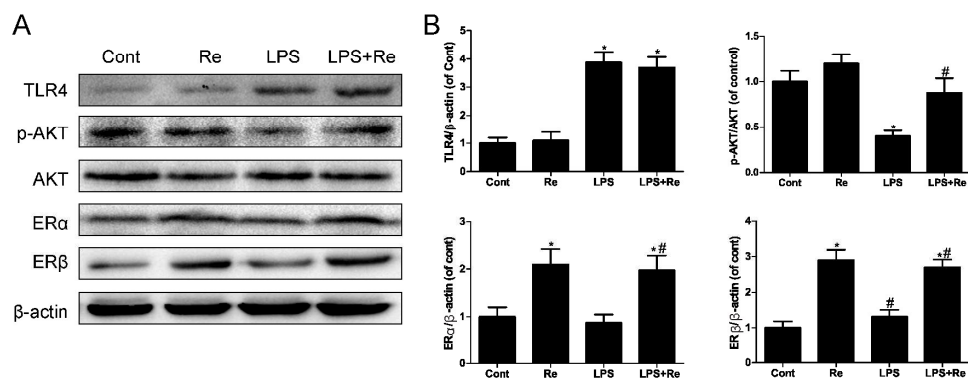
**Figure 6**

480

481

482

483

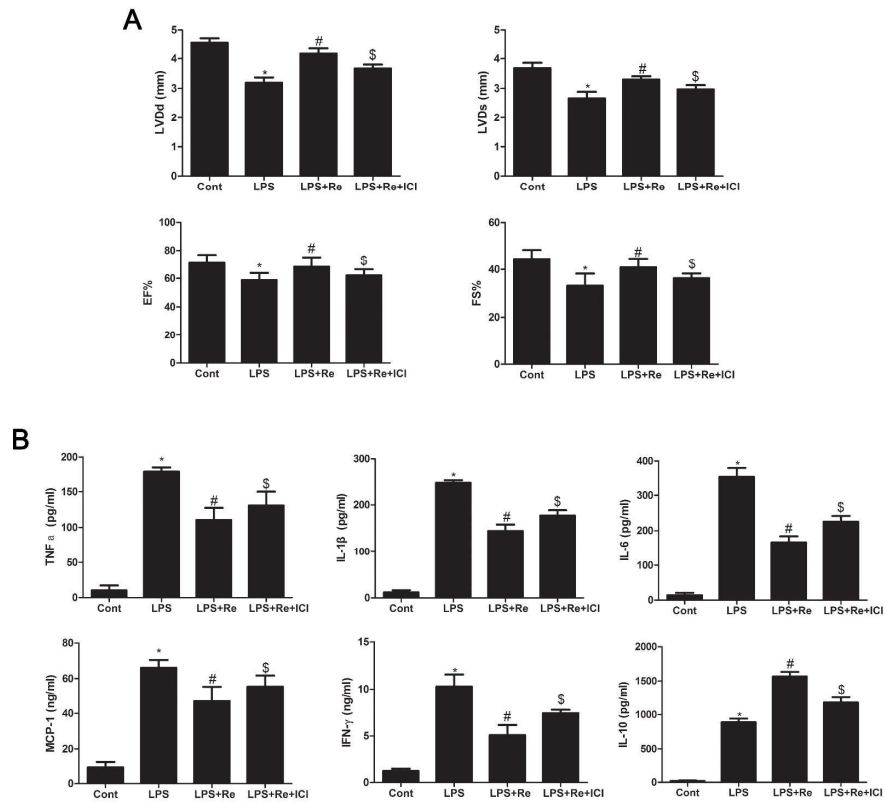
**Figure 7**

484

485

486

**Figure 8**



487

Ginsenoside Re protected against lipopolysaccharide-induced cardiac dysfunction in mice via ERs and PI3K/AKT mediated NFκB inhibition

